PDRFoam performance for flame acceleration in congested quiescent clouds

Josué Melguizo-Gavilanes[1], and Andrzej Pekalski[2]
[1] Shell Global Solutions B.V., Energy Transition Campus Amsterdam (ETCA)
Amsterdam, The Netherlands
[2] Shell Research Limited UK, Shell Center
London, United Kingdom

1 Introduction

An explosion is a rapid combustion process where flammable gases/dust/droplets ignite, creating burnt products that drives unburnt gases ahead of the flame. This interaction with obstacles generates turbulence, increasing flame speed and area in a positive feedback loop known as the Schelkin mechanism. Predicting gas explosion consequences in petrochemical plants is crucial for risk assessment and mitigation. Simple screening methods exist (e.g., CAM and SCOPE) but detailed predictions in complex geometries require CFD tools. These tools face challenges due to varying obstacle scales and complex combustion dynamics, necessitating a hybrid computational approach. The Porosity Distributed Resistance (PDR) method addresses these challenges by treating small obstacles as sub-grid elements and resolving large obstacles in full-scale simulations. Existing tools like FLACS, EXSIM, McNEWT-PDR, and COBRA use the PDR concept, but they lack capabilities such as explicit flame area transport and latest laminar/turbulent burning velocity correlations, and face some challenges in modeling the effects of explosion in adjacent congested regions with separation between them. See Puttock et al. [1] and references therein for a complete perspective on the method. PDRFoam, has been developed by Shell as an open-source tool that overcomes these limitations. Its performance has been assessed recently for vented hydrogen deflagrations [2] and hydrocarbon vapor cloud explosions [3]. Here, the flame acceleration dynamics in partially congested clouds is evaluated.

2 Numerical methodology

2.1 Solver description

Unsteady Favre-averaged equations for mass, momentum, enthalpy (unburnt and burnt) and regress variable together with porosity-modified standard $k-\epsilon$ turbulence model are employed; transport equations for the flame wrinkling parameter are also solved. Note that the PDR formulation introduces additional source terms in the momentum and turbulence equations, readers are referred to [1] for a detailed description of the physical, turbulence, combustion and subgrid models used.

Correspondence to: J.MelguizoGavilanes@shell.com

2.2 Domain, initial and boundary conditions

The computational domain is a rectangular cuboid of length $x = L$, width, $y = W$ and height $z = H$. The congestion is always placed at $(0, 0, 0)$ inside a 360 m^3 (20-m long, 6-m wide, 3-m high) homogeneous flammable cloud of stoichiometric ethane-air at ambient temperature and pressure ($T =$ 300 K; $p =$ 100 kPa). The mesh is uniform within the cloud with cell size, $cw = 0.3 - 0.46$ m depending on the congestion type, and it expands uniformly in all directions to save computational time. The domain boundaries are placed far away from the congestion and flammable cloud to avoid them having an effect on the flame acceleration dynamics. As for boundary conditions, zero gradient for scalars and velocity at the left/right, front/back and top face of the domain, and non-slip for velocity at the bottom face. Figure 1 shows an example of the numerical setup.

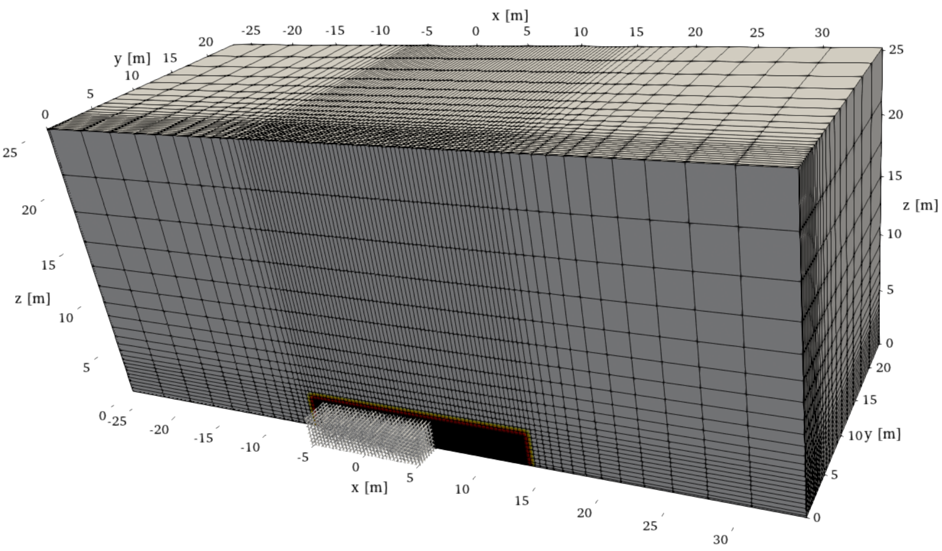

Figure 1: Domain clip at $y = 0$ showing initial conditions in flammable cloud.

The four congestion types used are shown in Figure 2, clockwise from the top left corner: (i) 3-D congestion, 5.2-m long; (ii) 3-D congestion, 10.4-m long; (iii) 2-D congestion (no pipes along the x-axis), 10.4-m long; (iv) 1-D congestion (no pipes along x- and y-axes), 10.4-m long. All rigs are nominally 5.2-m wide, and 2.6-m high, composed of 76-mm diameter pipes arranged at a pitch of 342 mm (distance between consecutive pipe centers).

Finally, before execution of PDRFoam, it is necessary to generate PDR fields of sub-grid parameters such as volume blockage, area blockage, and number of obstacles in each computational cell. A pre-processing script called CADPDR takes a description of CAD geometry consisting of a list of primitives (i.e. rectangular blocks, cylinders, etc.) and generates the necessary fields. One of the functions of the pre-processor is to record cells and faces totally blocked by obstacles so that these cells are removed from the mesh. See [1] for additional details.

2.3 Validation against Pekalski et al. [4]

To assess the performance of the PDR methodology to capture the flame speeds and overpressures developed during acceleration within the congestion (i), a comparison against the experimental data in [4] is carried out. The flame is ignited at $x = -2.6$ m (left end of the rig), and propagates towards $x = 2.6$ m (the right end of the rig). Figure 3 shows the pressure histories collected along the centerline $(x, 0, 0)$ for

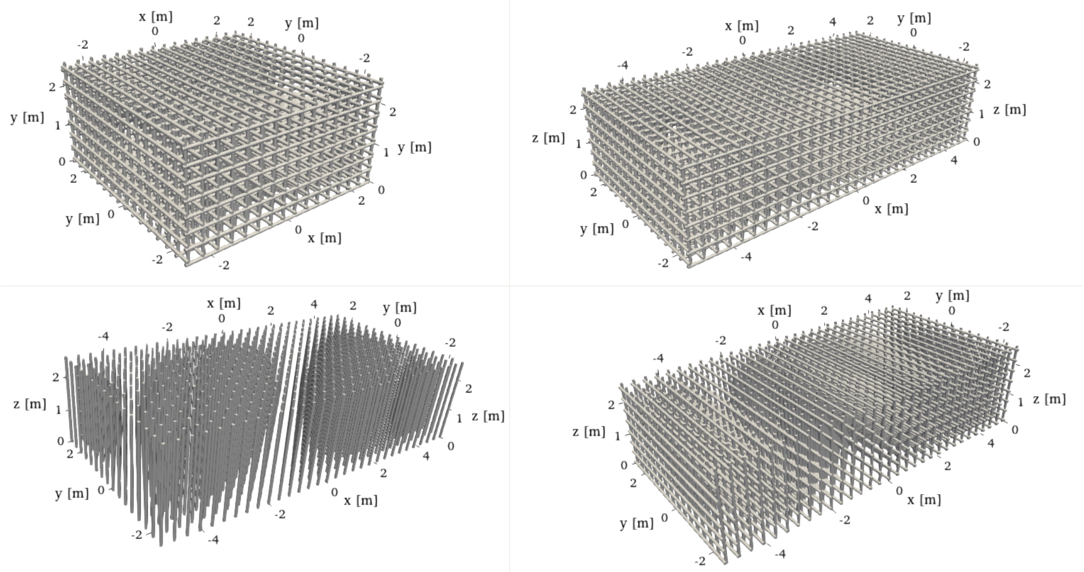

Figure 2: Schematic of congestion types considered.

different cell sizes cw; the actual axial locations are displayed on the subplots. The horizontal dashed lines plotted for $-2.6 \leq x \leq 2.6$ denote the experimentally measured pressure maxima at the given location. Overall, for $0.3 \leq cw \leq 0.4$ the overpressures are satisfactorily predicted throughout the rig, with some discrepancies observed at $x = -2.6$ m, and $x = 0.02$ m. Note that the CADPDR pre-processing script offers the possibility of automatic determination of the cell size based on an *a priori* analysis of the CAD file. In this case, $cw = \mathrm{Auto} = 0.3846$ m, which displays a more sensible behavior once the flame leaves the congestion ($x > 2.64$ m), i.e., with a less abrupt decay. In terms of flame speeds the agreement is also decent; the latter were computed based on time of arrival at the different pressure transducer locations. In [4], transition to detonation was reported in the unobstructed section of the flammable cloud. PDRFoam is not expected to recover this behavior since it lacks a detonation model, and congestion is needed to sustain high burning rates. This last observation, and the overall agreement with the experiment, motivates investigating the solver behavior for longer rigs of different types. Is the sensitivity of the solver to congestion type as that experimentally observed? Will the flame exhibit a change of combustion regime akin to DDT? Do the front velocities saturate to detonation like values? These questions are addressed in the next section.

3 Results

3.1 Flow fields

Figure 4 shows selected frames for rigs (ii), (iii) and (iv) which were described in subsubsection 2.2; $cw = \mathrm{Auto}$ is used to compute these cases which yield cell width values of 0.2985 m, 0.3508 m, and 0.4651 m for the 3-D, 2-D and 1-D congestion, respectively. The contours, colored by pressure, show the flame surface; red areas denote high-pressures. The flammable cloud is shown as a dark region engulfing and extending beyond the congestion. Note how the expansion of the flame pushes the reactive gas outside of the congestion, and the tip of the flame surface builds-up in pressure as it propagates. The gas ahead of the flame in turn interacts with the congestion generating turbulence that enhances the combustion rate in the resolved/unresolved part of the mesh. The expectation from experimental observation is for the flame that is ignited within the 3-D congestion to traverse the rig faster, than the

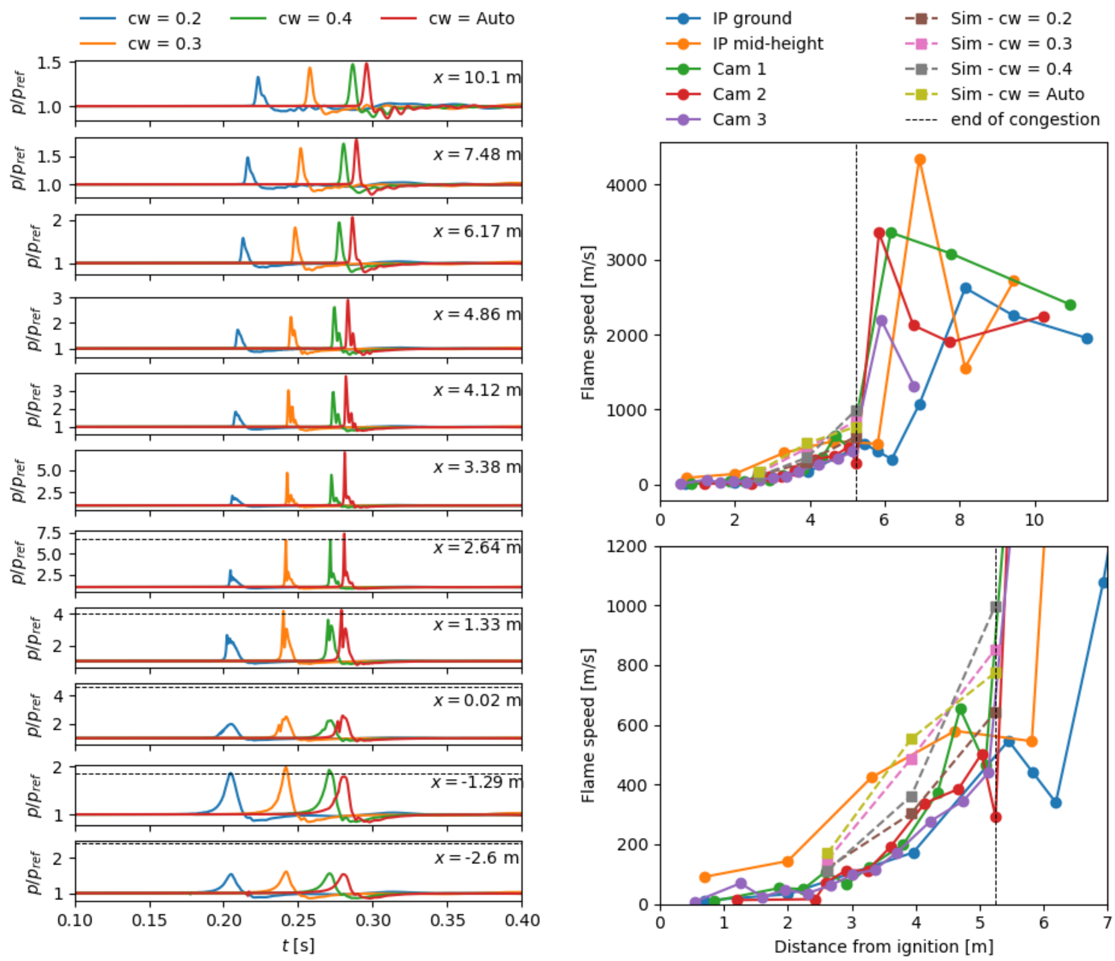

Figure 3: Pressure traces along congestion and cloud; horizontal dashed lines denote pressure maxima measured at probe locations. Flame speed within congestion.

2-D and 1-D congestion. This is indeed what PDRFoam reproduces. The flame reaches the end of the congestion at 0.242 s, 0.318 s and 0.425 s, respectively.

3.2 Pressure probes

Pressure histories and the pressure maxima recorded at the transducer locations are shown in Figure 5. The congestion is located at $-5.2 \leq x \leq 5.2$. Other than the differences in time of arrival already reported, the pressure histories indicate the appearance of shocks around $x = 0$ for the 3-D and 2-D congestion, and as $x \rightarrow 5.2$ m for the 1-D congestion. The pressure build-up as a function of distance is also quantified, the differences are measurable but minor during early stages of propagation for the 2-D and 3-D congestions, whereas the overpressure for the 1-D congestion is expectedly less than that reported for the other rigs. A figure of merit to assess the pressure levels attained during flame acceleration within the rig is the Chapman-Jouguet pressure which for a stochiometric ethane-air mixture is $p_{\mathrm{CJ}}/p_{\mathrm{ref}} = 17.3$. Since the reactive front is subjected to losses due to expansions at the edge of the reactive cloud during its propagation, this ratio provides an upper limit. The p/p_{ref} maxima at the end of the 3-D and 2-D congestion at the probe location is about 30% less than $p_{\mathrm{CJ}}/p_{\mathrm{ref}}$, and would be indicative of detonation like conditions. Interestingly, monitoring the pressure maxima over the entire

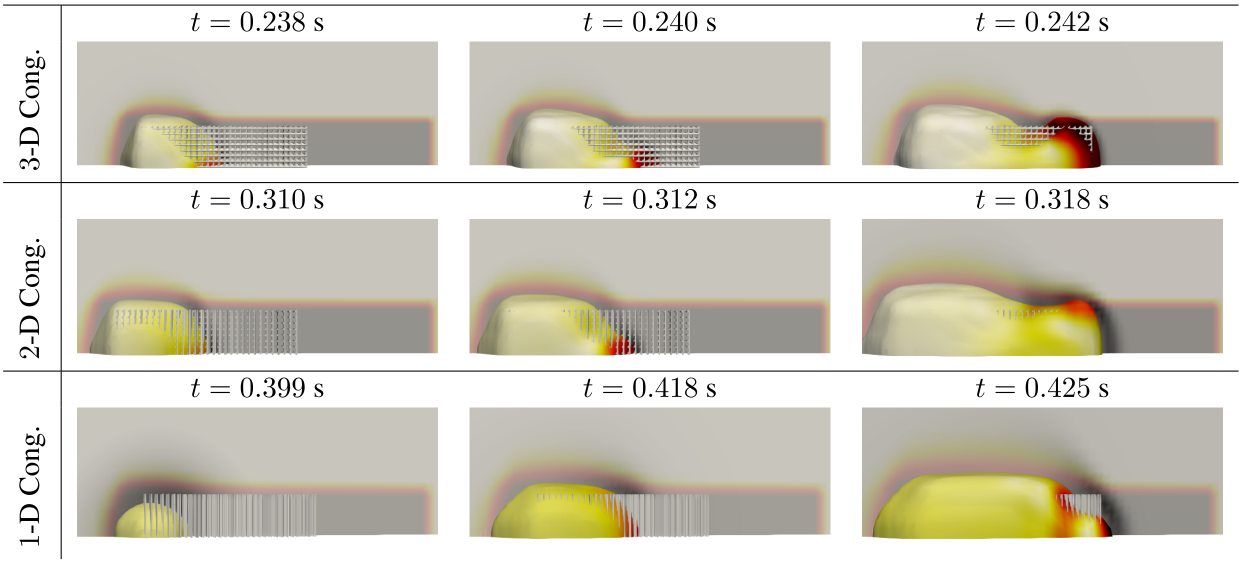

Figure 4: Selected frames showing the flame acceleration dynamics through 1-D, 2-D and 3-D congestion.

computational domain (not shown) yields values of $p_{\mathrm{CJ}}/p_{\mathrm{ref}} = 16.8$ at $t = 0.242$ s, 14.2 at $t = 0.316$ s and 7.2 at $t = 0.424$ s for the 3-D, 2-D, and 1-D congestions, respectively, which may suggest that a change in propagation regime could have indeed taken place within the rig.

3.3 $x - t$ and $u - x$ diagrams

The change in propagation regime alluded to earlier is substantiated by extracting position-time ($x - t$) diagrams from the simulation results, and computing front velocities that can be plotted as a function of distance ($u - x$ diagrams). These are shown in Figure 5 normalized by time of arrival at the end of the congestion, and half the rig's length. Note the presence of the two distinct peaks for the 3-D and 2-D congestion attaining values larger than the Chapman-Jouguet speed, $D/D_{\mathrm{CJ}} = 1$ ($D_{\mathrm{CJ}} = 1803$ m/s), plotted as a red horizontal dashed line for reference, and subsequently relaxing to sub-D_{CJ} values of $D/D_{\mathrm{CJ}} = 0.924$ ($D = 1666$ m/s), and $D/D_{\mathrm{CJ}} = 0.806$ ($D = 1453$ m/s) in the last meter of the congestion. The associated velocity deficits are 7.6% and 19.4% for the 3-D and 2-D congestions, respectively. The deficit reported for the 3-D congestion is a compelling sign that the PDR methodology as implemented in PDRFoam solver seems to be capable of capturing DDT events.

4 Conclusions

PDRFoam was assessed to capture the flame acceleration dynamics in partially congested flammable clouds. A satisfactory validation of the overpressures and flame velocities measured experimentally at large-scale was carried out. Subsequently, 1-D, 2-D, and 3-D congestion cases were computed to determine whether the solver was able to reproduce the sensitivities to congestion type, and a change of combustion regime akin to DDT. PDRFoam exceeded expectations. Future work will include a thorough validation against fully congested clouds in which DDT events are experimentally reported.

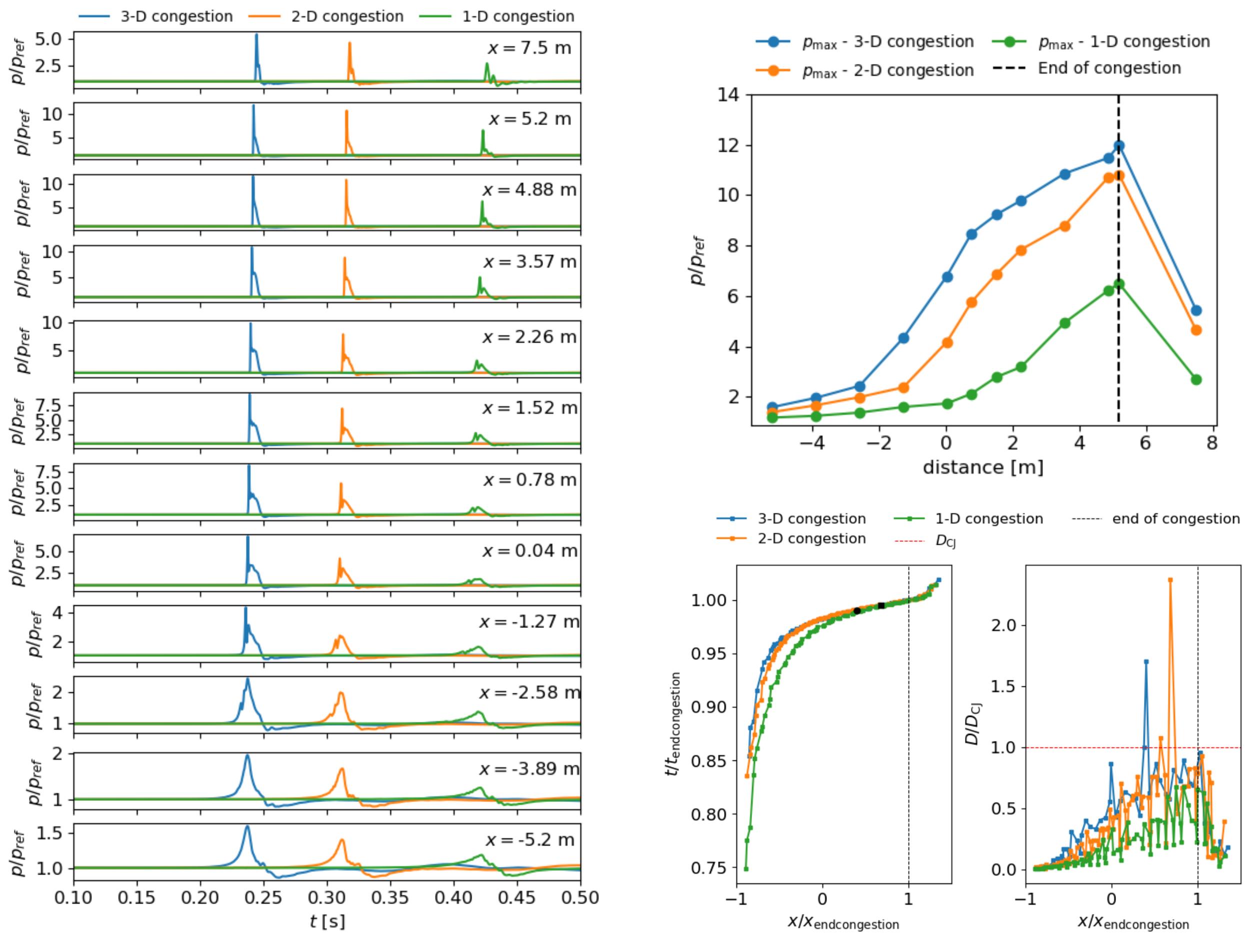

Figure 5: Left: Pressure histories along congestion and cloud. Right: pressure maxima recorded at probe locations, and $x - t$ and $u - x$ diagrams for different congestion types. Black markers denote time and location where change of propagation regime takes place.

References

[1] J. Puttock, F. Walter, D. Chakraborty, S. Raghunath, and P. Sathiah, "Numerical simulations of gas explosion using porosity distributed resistance approach part-1: Validation against small-scale experiments," *Journal of Loss Prevention in the Process Industries*, vol. 75, p. 104659, 2022.

[2] A. Zambare, V. D. Narasimhamurthy, T. Skjold, and H. Hisken, "Modelling of vented hydrogen deflagrations in an ISO container using PDRFoam," *International Journal of Hydrogen Energy*, vol. 59, pp. 251–262, 2024.

[3] M. Dhiman, A. Zambare, P. Sathiah, and V. D. Narasimhamurthy, "CFD simulations of vapour cloud explosions using PDRFoam," *Journal of Loss Prevention in the Process Industries*, p. 105164, 2023.

[4] A. Pekalski, J. Puttock, and S. Chynoweth, "Deflagration to detonation transition in a vapour cloud explosion in open but congested space: Large scale test," *Journal of Loss Prevention in the Process Industries*, vol. 36, pp. 365–370, 2015.